

# *EARTHQUAKE ENGINEERING PRACTICE*

## **Assessment of Performance-Based Seismic Design Methods in ASCE 41 for New Steel Buildings: Special Moment Frames**

John Harris,<sup>a)</sup> M.EERI, and Matthew Speicher,<sup>a)</sup> M.EERI

This paper presents the results of a study investigating the correlation between the anticipated seismic performance of an *ASCE 7* code-compliant steel building with special moment frames and its predicted performance as quantified using *ASCE 41* analysis procedures and structural performance metrics. Analytical results based on component-level performances at the collapse prevention structural performance level indicate that special moment frames designed in accordance with *ASCE 7*, and its referenced standards, have difficulty satisfying the acceptance criteria in *ASCE 41* for an existing building intended to be equivalent to a new building. [DOI: 10.1193/050117EQS079EP]

### INTRODUCTION

In 1997, the Federal Emergency Management Agency (FEMA) published FEMA 273 (FEMA 1997) as a first step towards standardizing seismic performance assessment procedures for existing buildings. This effort, produced under the Applied Technology Council's Project 33, was the first significant step in implementing performance-based seismic design (PBSD) into practice. Subsequently, in 2000, FEMA and the American Society of Civil Engineers (ASCE) published FEMA 356 (FEMA 2000a). This publication introduced many changes to FEMA 273 to refine the accuracy and applicability of the provisions. Motivation for the movement toward PBSD is discussed in these aforementioned documents. In 2006, the ASCE published *ASCE/SEI 41-06* (ASCE 2007) as an ASCE Standard—hereafter referred to as *ASCE 41*, which was updated in 2013 (*ASCE/SEI 41-13*; ASCE 2014); the next update (*ASCE/SEI 41-17*; ASCE 2017) is scheduled for publication in late 2017.

*ASCE 41* represents the current state-of-the-practice in seismic evaluation and retrofit of existing buildings. This standard is referenced for use by the 2012 *International Existing Building Code* (IEBC; ICC 2012a), the California Building Standards Code (CBSC 2010), federal government building standards and guidelines (e.g., NIST 2011, NIST 2017a), and several other local jurisdictions. *ASCE 41* provides analytical procedures and performance criteria for evaluating buildings and designing seismic retrofits based on a defined performance objective. This ability to explicitly define a performance goal

---

<sup>a)</sup> National Institute of Standards and Technology, 100 Bureau Drive, Gaithersburg, MD 20899; Email: john.harris@nist.gov (JH, corr. author)

and then assess a building design against that goal has led some practitioners to adapt *ASCE 41* methodology for use in new building design. The performance-based methodologies in *ASCE 41* provide an alternative to the traditional prescriptive approaches used in the current standard for new buildings, *ASCE/SEI 7-10 (2010)*—hereafter referred to as *ASCE 7*. Referenced for use by the 2012 *International Building Code (IBC; ICC 2012b)*, *ASCE 7* is widely used throughout the United States for seismic design of new buildings.

Although *ASCE 7* allows PBSB to be used in new building design, it provides no substantial guidance on implementing PBSB for this purpose. Therefore, practitioners and local authorities have turned to the provisions in *ASCE 41* as a way of implementing PBSB into new building design. For example, PBS-P100 (*GSA 2012*) prescribes that *ASCE 41* shall be used for the seismic design of new GSA facilities and that the guidelines from *ASCE 41* are intended to be applied to new buildings. The National Institute of Building Sciences (NIBS) is using PBS-P100 as the basis for developing their *National Performance-Based Design Guide (NIBS 2013)*. Further, *ASCE/SEI 7-16 (2016)* includes expanded provisions regarding nonlinear response history analysis that reference the use of *ASCE 41* for modeling and acceptance criteria for structural components.

Though provisions in *ASCE 41* were originally intended to be used in the evaluation of existing buildings, *ASCE/SEI 41-13 (2014)* offers a new track for application of the provisions to existing buildings whose performance goal is selected to be equivalent to that of a building designed with the new building standard, *ASCE 7*. Consequently, this new track allows direct seismic performance assessment of new buildings using *ASCE 41*. However, the correlation between the performance of a building designed with the prescriptive provisions of *ASCE 7* and performance resulting from an assessment using the performance-based provisions of *ASCE 41* is largely unknown. *ASCE 41* does not provide a direct correlation between its rehabilitation objectives and the intended performance of an *ASCE 7* code-compliant building. However, the IEBC does provide a correlation between the performance levels of *ASCE 41* and risk categories of *ASCE 7*, thus providing a qualitative link between the prescriptive requirements for new building design and the nonprescriptive requirements of existing building assessment. This linkage has not been comprehensively validated nor have the seismic performance expectations for new buildings been quantitatively assessed to standardize acceptable performance within the framework of *ASCE 41*, or vice versa.

This paper presents the results of a study investigating the correlation between the anticipated seismic performance of an *ASCE 7* code-compliant steel building with special moment frames (SMFs) and its predicted performance as quantified using *ASCE 41* analysis procedures and structural performance metrics. The goals of this project are as follows:

- Assess *new* structural steel buildings utilizing SMFs designed per *ASCE 7* requirements and, in turn, evaluated using *ASCE 41*,
- Develop a qualitative link between the performance anticipated in *ASCE 7* considering the performance identified by *ASCE 41* procedures and performance measures,
- Provide guidance or technical support for improved or new provisions in *ASCE 41* (and, to a lesser extent, *ASCE 7*), and
- Identify and reduce any inconsistencies, ambiguities, or confusing provisions in *ASCE 41*.

The basic question is whether the standards for designing new steel buildings and assessing existing steel buildings provide consistent levels of performance. For brevity, only assessment results for the collapse prevention structural performance level will be shown in this paper. A complete project report is provided in [Harris and Speicher \(2015a\)](#). Results from the same study concerning other building systems can be found in [Harris and Speicher \(2015b, 2015c\)](#) and [Speicher and Harris \(2016a, 2016b, 2017\)](#).

### APPLICABILITY OF *ASCE/SEI 41-13* AND *ASCE/SEI 41-17* TO THIS STUDY

This project was initiated using [ASCE/SEI 41-06 \(2007\)](#) as its basis. During the project, [ASCE/SEI 41-13 \(2014\)](#) completed committee review and was published in 2014. As such, new or updated provisions in [ASCE/SEI 41-13 \(2014\)](#) were not incorporated, except where changes were required to align with the seismic hazard prescribed in [ASCE/SEI 7-10 \(2010\)](#). Regarding assessment of structural steel components, the technical content in [ASCE/SEI 41-13 \(2014\)](#) did not change in any significant manner that invalidates the results presented in this paper.

As of early 2017, the *ASCE 41* committee has nearly finished balloting proposed provisions for [ASCE/SEI 41-17 \(2017\)](#). A significant effort was made this code cycle to bring the provisions for evaluation of structural steel components, particularly those found in moment frames, to the state-of-the-art (and state-of-the-practice) and align with standard steel design provision where needed. Specific changes in [ASCE/SEI 41-17 \(2017\)](#) could affect the results presented in this paper—a future paper is planned to show those changes.

### ARCHETYPE STEEL BUILDINGS

Six steel frame office buildings to be constructed in an area of high seismicity are designed in accordance with *ASCE 7*. The building suite consists of three building heights: 4-, 8-, and 16-story. Each building is rectangular in plan, with overall plan dimensions of 152 feet [46 m] by 102 feet [31 m]. Floor-framing bays and dimensions are shown in [Figure 1](#). For all buildings, the height of the first story is 18 feet [5.5 m], and the remaining story heights are 14 feet [4.3 m]. Building stability and resistance to environmental loads and deformations are provided by SMFs along the east-west (E-W) direction and special concentrically braced frames (SCBFs) along the north-south (N-S) direction. All seismic force-resisting systems (SFRSs) are symmetrically located at the perimeter of the building and orthogonal. This paper focuses only on the moment frames. More information regarding the archetype building designs can be found in [Harris and Speicher \(2015a\)](#).

The buildings are analyzed and designed for all load effects in accordance with the 2012 IBC and its referenced standards: [ASCE/SEI 7-10 \(2010\)](#), [ANSI/AISC 360-10 \(2010a\)](#), [ANSI/AISC 341-10 \(2010b\)](#), and [ANSI/AISC 358-10 \(2010c\)](#). The following material types were assumed in design: A992 ([ASTM 2015a](#)) for wide-flange sections, A500 Grade B ([ASTM 2013](#)) for hollow structural sections, and A572 Grade 50 [345] ([ASTM 2015b](#)) for connection components.

Floor and roof dead load consists of the weight of the steel members, metal deck, and concrete slab (3 1/4-inch [83-mm] lightweight concrete at 110 pcf [1760 kg/m<sup>3</sup>] on 18-gauge, 3-inch [76-mm] metal deck  $\approx$  46 psf [2.2 kPa]). Superimposed dead loads are taken as 15 psf [0.7 kPa] for floors and 10 psf [0.5 kPa] for the roof, representing mechanical,

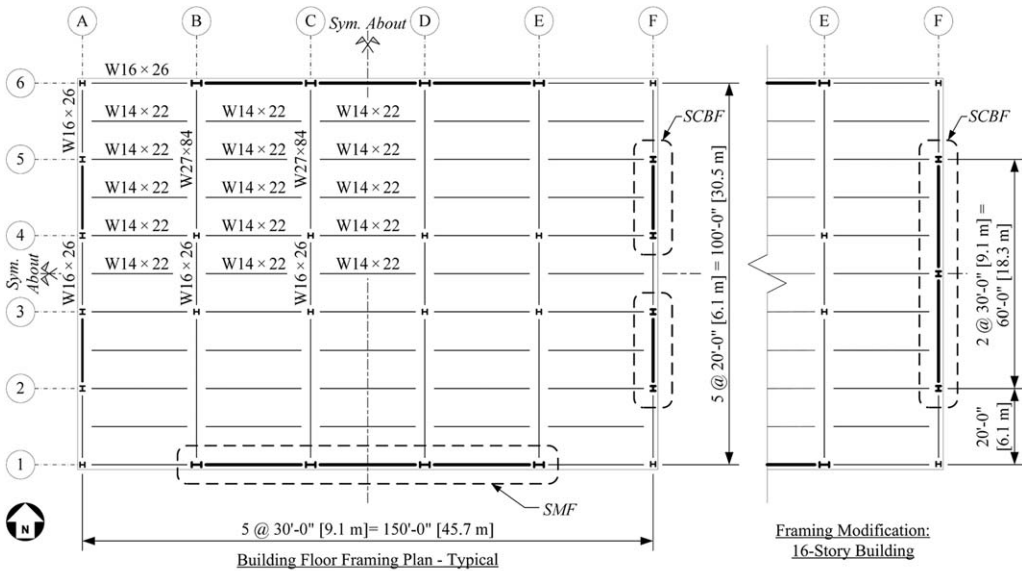


**Figure 1.** Typical floor framing plan for each archetype building.

electrical, plumbing, and miscellaneous dead load. A 250 lbs per foot [372 kg/m] superimposed dead load is applied to the perimeter horizontal framing at each floor to account for façade weight. The design live load is 50 psf [2.4 kPa] for floors and 30 psf [1.4 kPa] for the roof.

For design for earthquake effects, two designs are produced for each building height to determine the equivalent seismic effects: (1) using the equivalent lateral force (ELF) procedure and (2) using the modal response spectrum analysis (RSA) procedure. Effective seismic weights for computing the horizontal earthquake forces are determined from dead loads plus 20% of the unreduced design floor live loads. The story gravity loads for seismic drift analysis (including period calculation) and stability verification are determined from dead loads plus 25% of the unreduced floor live loads. Roof live loads are considered not to be present for seismic drift analysis. Allowable seismic drift limit is set to  $h_{sx}/50$ , where  $h_{sx}$  is the story height below the level under consideration.

The following parameters summarize the seismic hazard prescribed in *ASCE 7* for design:

- Building Risk Category: II
- $S_S = 1.5 g$ ,  $S_1 = 0.599 g$
- Site Soil Conditions: Site Class D, Stiff Soil
- $S_{DS} = 1.0 g$ ,  $S_{D1} = 0.599 g$
- Seismic Design Category (SDC): D

$S_S$  and  $S_1$  are the mapped  $MCE_R$ , 5% damped, spectral response acceleration parameters in terms of the acceleration of gravity,  $g$ , at short periods and at a period of 1 s, respectively.  $S_{DS}$  and  $S_{D1}$  are the 5% damped design spectral response acceleration parameters at short

periods and at a period of 1 s, respectively. The seismic analysis and design parameters for each building along the E-W direction are shown in Table 1.

For design for wind effects, the basic wind speed is taken to be 110 mph [177 km/h] for the 700-year wind for strength design of components and 72 mph [116 km/h] for the 10-year wind for verifying story drifts (serviceability). The allowable wind drift limit is set to  $h_{sx}/400$ . The same gravity load combination used for the seismic drift analysis is used in the wind drift analysis. Consequently, some components of the SFRS may include significant overstrength to resist nonseismic loads or to satisfy other design criteria.

The SMF designs for all frames are shown in Figure 2. Each frame schematic shows the ELF design (left side) and RSA design (right side).

### SEISMIC ASSESSMENT

A structural seismic performance assessment of the SMFs is conducted using both linear and nonlinear analysis procedures as prescribed in *ASCE 41*:

- Linear Static Procedure (LSP)
- Linear Dynamic Procedure – Response Spectrum (LDP)
- Nonlinear Static Procedure (NSP)
- Nonlinear Dynamic Procedure (NDP)

The seismic performance target is selected as the Basic Safety Objective (BSO). This objective includes the interrelated goals of Life Safety (LS) Structural Performance Level (SPL) at the Basic Safety Earthquake-1 (BSE-1) earthquake hazard level (EHL) and Collapse Prevention (CP) SPL at the BSE-2 EHL. For the BSO, the BSE-2 EHL is taken equal to the maximum considered earthquake ( $MCE_R$ ) defined by *ASCE 7* and the BSE-1 EHL is taken equal to two-thirds of the BSE-2 EHL. This selection allows the correlation between the intended seismic performance objective of *ASCE 41* and the intended design objective of *ASCE 7* for an *ordinary* building to be evaluated, which is qualitatively defined here as “life safety” provided by collapse prevention of the building given an  $MCE_R$  event. Nonstructural Performance Levels are not considered in this study. Results from assessment for the CP SPL are presented in this paper; information regarding other performance levels can be found in [Harris and Speicher \(2015a\)](#).

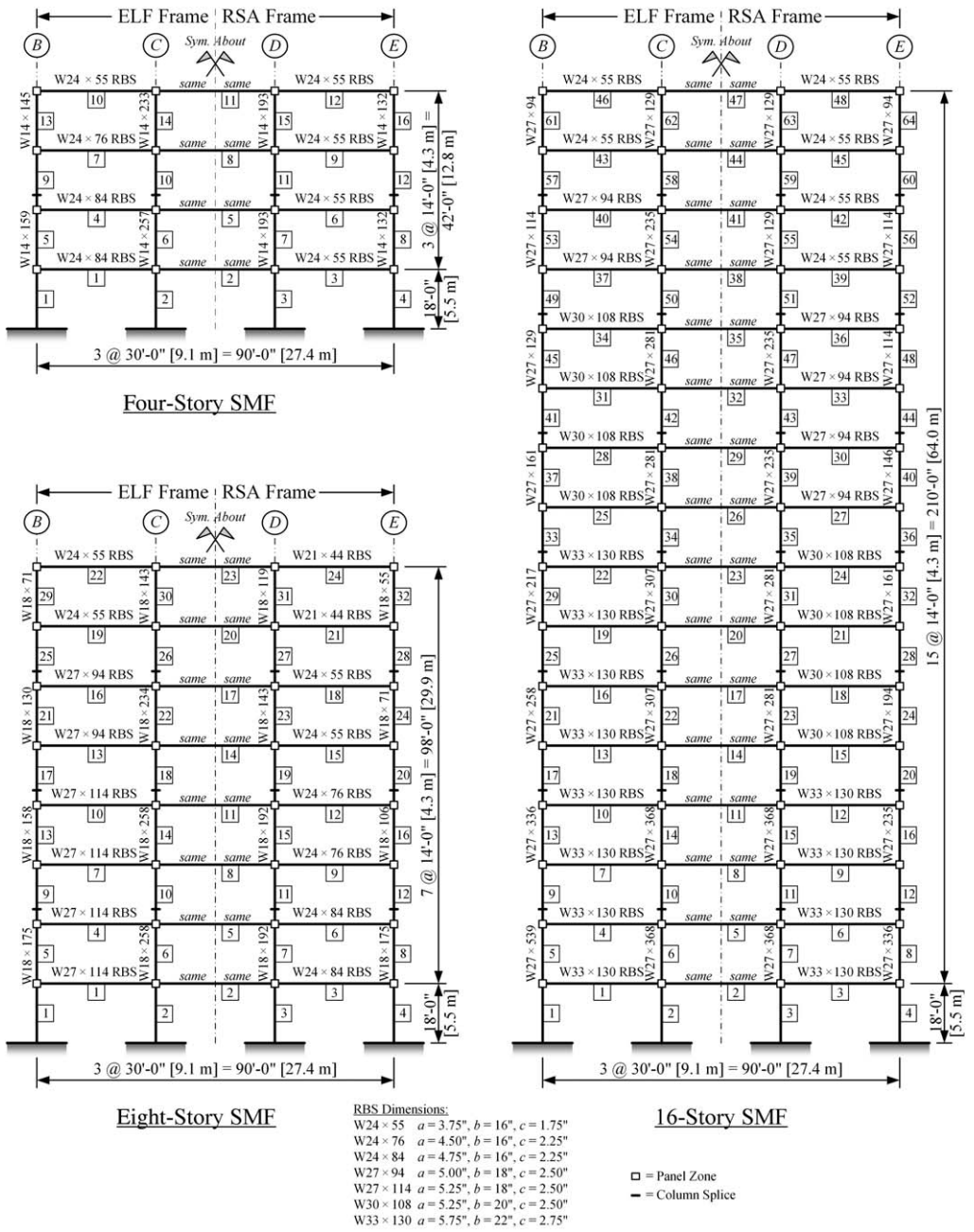
The following parameters summarize the seismic hazard prescribed in *ASCE 41* for assessment at the BSE-2 EHL:

- $S_S = 1.5 g$ ,  $S_1 = 0.599 g$
- Site Soil Conditions: Site Class D, Stiff Soil
- $S_{XS} = 1.5 g$ ,  $S_{X1} = 0.899 g$

$S_{XS}$  and  $S_{X1}$  are the 5% damped spectral response acceleration parameters at short periods and at a period of 1 s, respectively, for the desired performance level.

It is important to stress that prior to [ASCE/SEI 7-10 \(2010\)](#), the MCE was defined as a uniform seismic hazard associated with a 2% probability of being exceeded in 50 years, except near known faults where deterministic-based hazards controlled. [ASCE/SEI 7-10 \(2010\)](#) adopted a risk-targeted design philosophy that shifts from a uniform *hazard design*





Note: Steel member sizes provided in U.S. standard notation—see AISC (2011) for SI equivalents

Figure 2. Schematics of the SMF in each archetype building.

*basis* to a uniform *risk design basis*, and defines the MCE ground motion intensity (denoted as  $MCE_R$ ) as ground motions having a 1% probability of causing total or partial structural collapse in 50 years, except near known faults where deterministic-based hazards control. This risk has a conditional probability (“anticipated reliability”) of 10% probability of total or partial structural collapse conditioned on the occurrence of an MCE event. Several reference documents are available for more information about this implementation (ASCE 2010, FEMA 2009a, and NIST 2012).

In reference to developing a link between ASCE 7 and ASCE 41, the primary difficulty in equating the two standards is rooted in their disjointed performance objectives. That is, acceptance criteria for the CP SPL in ASCE 41 for structural components are not directly calibrated to the system-level seismic performance objective of ASCE 7. Consequently, the question becomes what percentage of components needs to fail the CP SPL to achieve a 10% probability of total or partial collapse given an  $MCE_R$  event?

All components of the SFRS are classified as *primary* components for both linear and nonlinear assessment procedures. Gravity framing (non-SFRS components) is assumed to provide negligible analytical lateral stiffness and strength. Therefore, non-SFRS components are classified as *secondary* components. Performance assessment of these secondary members is outside the scope of this study. Similar to the assumptions adopted for design, specific component stiffnesses (e.g., partially restrained composite shear tab connections and stairs) are not modeled explicitly in the mathematical model. This is done to minimize the influence of secondary components on the demands imposed on primary components, allowing assessment results between linear and nonlinear analysis to be compared.

The archetype buildings are modeled and analyzed in ETABS (Computers and Structures, Inc. [CSI] 2011a) for the linear procedures and PERFORM-3D (CSI 2011b) for the nonlinear procedures. A critical aspect of the NDP is the selection and scaling of input ground motions (free-field motions). For this study, the record set for each building consisted of 14 unique records. The selection methodology adopted and the record set used for each building, as well as specific parameters required for nonlinear static and dynamic analyses, are discussed in Harris and Speicher (2015a).

All nonlinear component actions are modeled with the anchor points (A to E) bounding the backbone curve shown in Figure 3 and quantified in ASCE 41. Component actions are calibrated based on experimental results to determine cyclic and in-cycle stiffness degradation only; post-yield strength increases and strength degradation were not calibrated but rather taken from ASCE 41. Information regarding the force-deformation calibration for moment frame components is provided in Harris and Speicher (2015a). Component strength at the ultimate deformation, point E on the backbone curve, retains the residual strength and does not experience complete strength loss.

## ACCEPTANCE CRITERIA

The acceptance criteria of a component action for a given SPL is satisfied when the force or deformation demand,  $Q_U$ , is less than or equal to an adjusted force or deformation capacity,  $Q_C$ . Component actions are classified as *force-controlled* or *deformation-controlled* depending on the post-elastic behavior of the component. Compliance with a performance

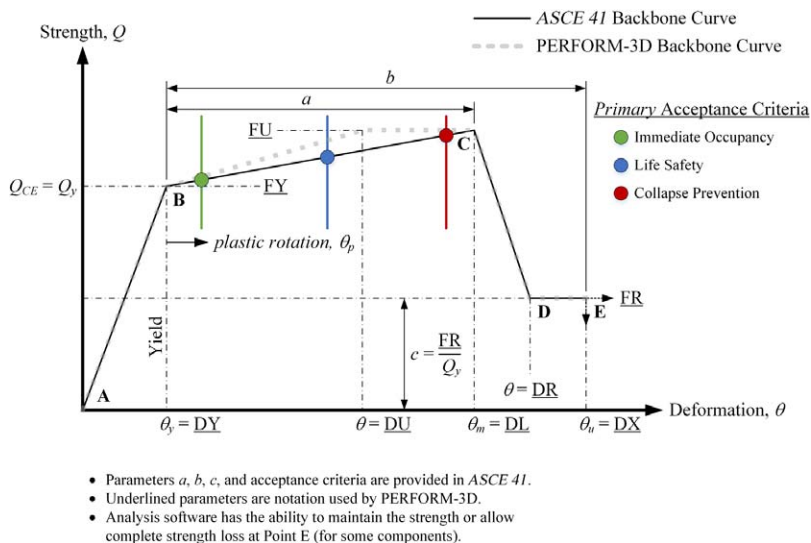


Figure 3. Generalized component backbone curve used in ASCE 41 and PERFORM-3D.

level is done in this study with a normalized demand-to-capacity ratio ( $DCR_N$ ) so that the acceptance criterion becomes a unity check similar to that done in modern component design standards. This approach is also a consistent way to present results over the various types of assessment procedures used in this study.

For linear assessment procedures,

$$\text{Deformation-controlled: } DCR_N = \frac{Q_{UD}}{m\kappa Q_{CE}} \tag{1}$$

$$\text{Force-controlled: } DCR_N = \frac{Q_{UF}}{\kappa Q_{CL}} \tag{2}$$

In Equations 1 or 2,  $Q_{UD}$  is the force demand on a deformation-controlled action,  $Q_{UF}$  is the force demand on a force-controlled action;  $m$  is the component demand modification factor (to account for the ductility associated with a specific action and depends on the SPL and component type);  $\kappa$  is the knowledge factor (taken as unity in this study to represent *new component capacities or actions*);  $Q_{CE}$  is the expected (mean) force capacity of a component; and  $Q_{CL}$  is the lower-bound (mean minus one standard deviation) force capacity of a component.

For nonlinear assessment procedures,

$$\text{Deformation-controlled: } DCR_N = \begin{cases} \text{Total} & \frac{\theta_{plastic} + \theta_{elastic}}{\kappa(\theta_y + \theta_{pe} + \theta_{p,AC})} \\ \text{Plastic} & \frac{\theta_{plastic}}{\kappa\theta_{p,AC}} \end{cases} \tag{3}$$

$$\text{Force-controlled: } DCR_N = \frac{Q_{UF}}{\kappa Q_{CL}} \text{ or } DCR_N = \frac{\theta_{total}}{\kappa \theta_y} \quad (4)$$

In Equations 3 or 4,  $\theta_{plastic}$  is the plastic deformation demand on a component,  $\theta_{elastic}$  is the elastic deformation demand on a component,  $\theta_y$  is the expected yield deformation capacity of a component,  $\theta_{pe}$  is the post-yield elastic deformation of a component,  $\theta_{p,AC}$  is the permissible plastic deformation capacity associated with a performance level for verifying the acceptance criteria, and  $\theta_{total}$  is the total deformation demand on a component. The choice of whether to use plastic or total deformations will depend on what force-deformation model is adopted for each component action in the structural analysis. Consequently, yield and post-yield elastic deformations may need to be added to the values given in *ASCE 41* to determine the total deformation for each SPL.

In this study, demands on *primary* components are compared with permissible force or deformation capacities for *primary* components. For nonlinear procedures, *ASCE 41* allows *primary* component demands to be within the acceptance criteria for *secondary* components if degradation effects are explicitly modeled—this allowance is neglected in this study.

The nonlinear analysis is carried out until the analysis routine fails to converge or an arbitrarily selected roof drift ratio of 20% is achieved. While both of these criteria are used to indicate and rationalize total or partial collapse of a system, the indicator of collapse used in this study is the  $DCR_N$  value for the CP performance level. Table 2 indicates the number of records out of 14 that did not complete the analysis at the BSE-2 EHL due to excessive lateral drift or solution nonconvergence.

## SMF ASSESSMENT RESULTS

Plots in this section present the  $DCR_N$  values for each SMF component for the CP SPL given the BSE-2 EHL. In lieu of parsing the figures by building, the figures are grouped by SMF component type: *beam-to-column connection*, *panel zone*, and *column*. A *beam* component is not evaluated because the flexural hinge develops in the beam-to-column connection.

The  $DCR_N$  values obtained from the LSP, LDP, NSP (push to right), and NDP are shown in each figure. Results for the NDP using the ground motion record set are statistically summarized by the median and mean (arithmetic). However, caution should be used when comparing linear and nonlinear results by inspection because the nature of the analysis is fundamentally different between them; presenting them together here is not intended to imply they are equivalent.

**Table 2.** Number of analyses that did not complete

Stories	ELF	RSA
4	0	5
8	3	10
16	0	4

### Beam-to-Column Connections

Figure 4 shows the performance of the beam-to-column connections (reduced beam section [RBS]) in terms of flexural response. The figure indicates that the many RBS connections fail the acceptance criteria. As is evident from the figure, connections in the ELF-designed frames perform better than those in the RSA-designed frames. Performance failures of the connections are generally associated with reduced permissible parameters attributed to panel zone strength, connection detailing, span-to-depth ratio, and section compactness. The section compactness requirements in *ASCE 41* match those prescribed for a highly ductile beam in *AISC 341*—though  $F_{ye}$  is used in *ASCE 41*. Therefore, the permissible parameters for the connections are generally not reduced for section compactness, as the

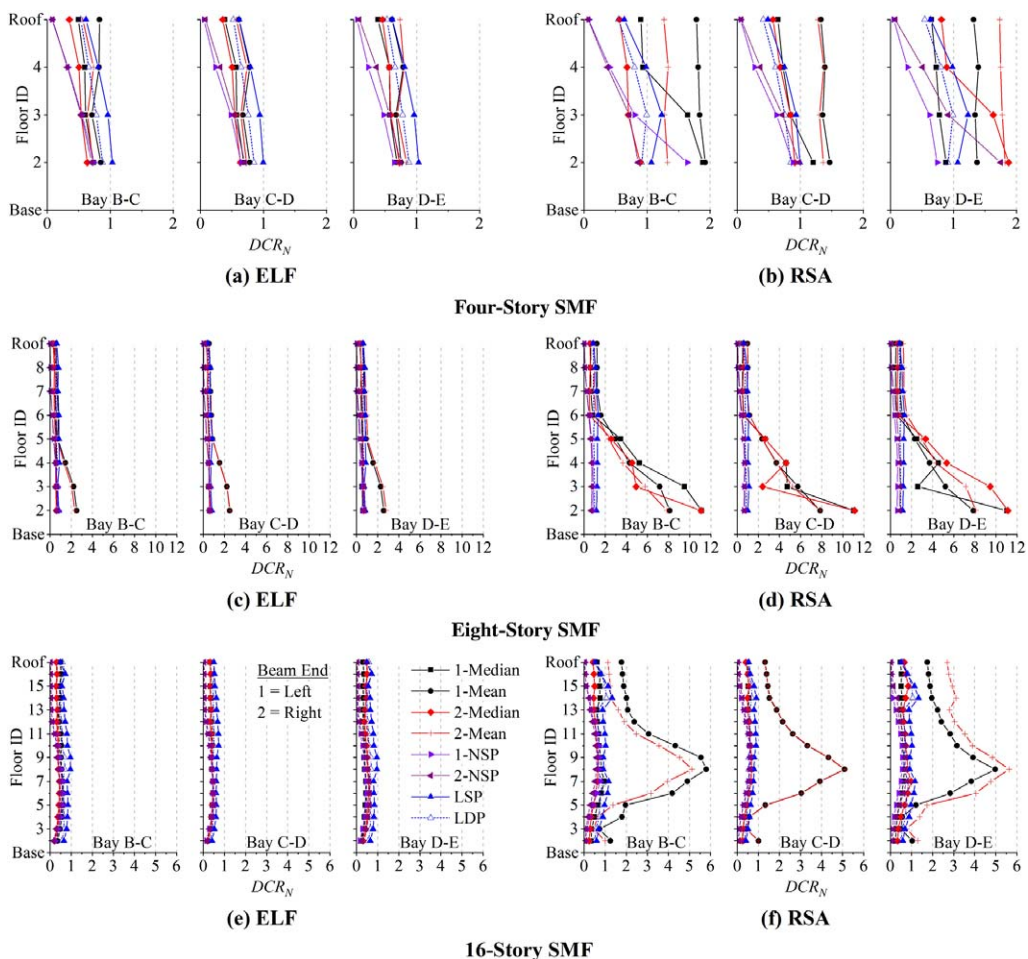


**Figure 4.** Assessment results for the beam-to-column connections for the CP SPL at the BSE-2 EHL for each archetype building: (a) MC4 ELF design; (b) MC4 RSA design; (c) MC8 ELF design; (d) MC8 RSA design; (e) MC16 ELF design; and (f) MC16 RSA design.

beams are designed with modern codes. Columns designed to meet the highly ductile section compactness requirements in *AISC 341* will generally require continuity plates to bypass the reduction on the permissible parameters. However, continuity plate thickness,  $t_{cp}$ , in one-sided connections do trigger a reduction in some connections, since *ASCE 41* requires  $t_{cp} \geq t_{bf}$  and *AISC 341* requires  $t_{cp} \geq t_{bf}/2$ , where  $t_{bf}$  is the thickness of the beam flange. Further, *AISC 358* requires that  $L_c/d_b \geq 7$  for an RBS connection, but *ASCE 41* requires a reduction on the permissible strengths using the linear procedures when  $L_c/d_b > 10$ , where  $L_c$  is the length of beam between columns and  $d_b$  is the depth of the beam. In many cases in this study, the span-to-depth ratio criterion triggered a reduction to the linear criteria but not similarly to the nonlinear criteria, as a reduction is required for the nonlinear procedures when  $L_c/d_b < 8$ . Also, increasing column sizes to offset the need for doubler plates can be problematic with regard to the anticipated connection performance—see Panel Zones section later. Nonetheless, it is debatable if the formulations of these reductions, based on a cumulative step function, are appropriate for components expected to experience inelastic straining.

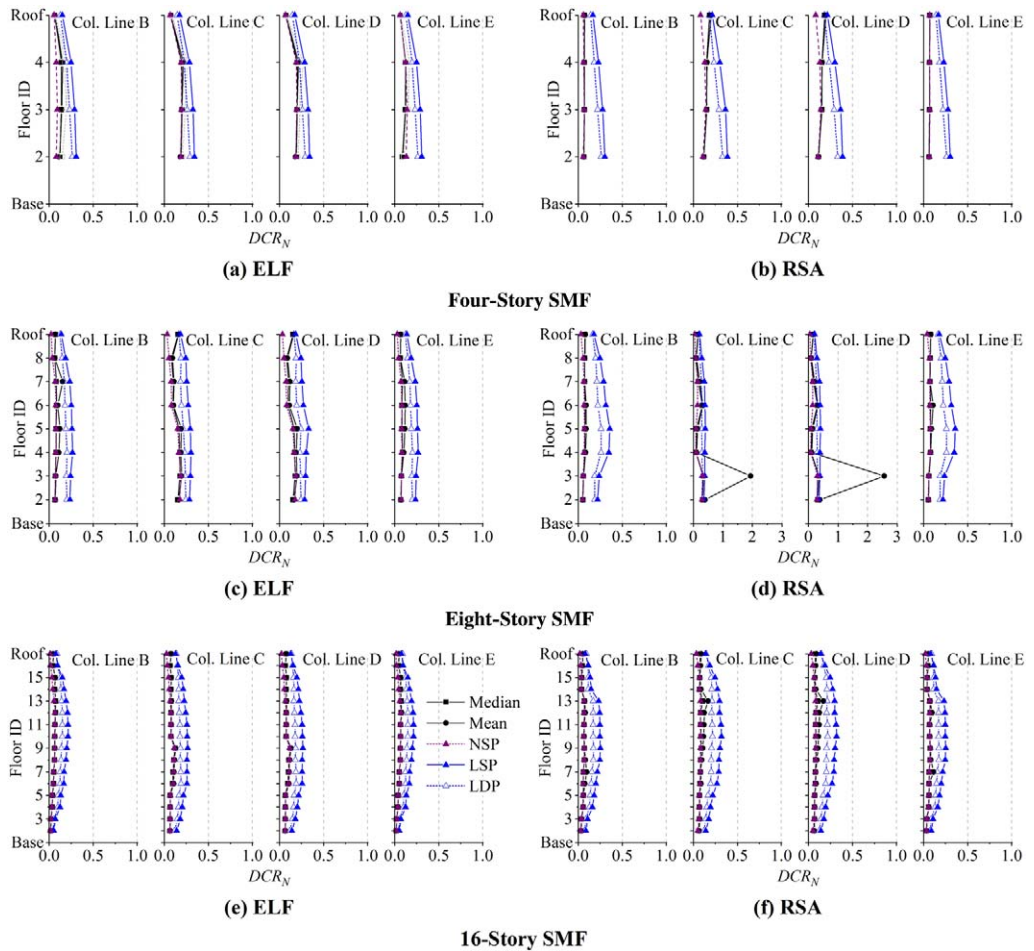
### Panel Zones

Figure 5 shows the performance of the panel zones in terms of shear response. As is evident from the figure, results indicate that the panel zones consistently satisfy the performance criteria. However, Figure 5d shows an anomaly in the interior panel zones on the third floor of the RSA-designed frame that is a direct effect of the response of the beam-to-column connections on that floor, shown in Figure 4d, and not a potential issue with the panel zones. Converting the results from the NDP to ductility demand indicates that the demands are consistently less than four times the shear yield strain,  $4 \times \gamma_y$ , which is the deformation at which the panel zone nominal strength is calculated (see Krawinkler 1978). These results show that the panel zones are stronger than required by the assessment criteria. This overstrength can be partly attributed to designing the panel zones for the *probable* connection strength in lieu of the first yield strength as recommended in FEMA 355D (FEMA 2000b) as well as upsizing column sizes to offset the need for doubler plates. As noted above, this increase in panel zone strength can impact the permissible capacities of the adjacent beam-to-column connection.

Take for example, a one-sided connection where a  $W24 \times 76$  [W610  $\times$  113] beam connects to a  $W18 \times 106$  [W460  $\times$  158] column. The ratio of shear in the panel zone at the probable flexural strength of the connection,  $V_{pr}$ , as calculated from *AISC 358*, to shear yielding of the panel zone,  $V_y$ , as calculated from *ASCE 41*, is 0.98 ( $F_y = 50$  ksi [345 MPa]). This result indicates that the panel zone may not yield until the connection approaches its peak flexural strength. For this example, the ratio of  $V_{PZ}/V_y$  is 0.74, where  $V_{PZ}$  is the shear in the panel zone corresponding to the first yield flexural strength of the RBS.

### Columns

Figure 6 shows the performance of the column hinges in terms of flexural response. For the linear procedures, section strength and member strength of a column are combined into a single axial-moment ( $P - M$ ) interaction equation in *ASCE 41*. For the nonlinear procedures, the plastic hinge is explicitly modeled using a  $P - M$  yield surface. While *ASCE 41* addresses flexural hinges in columns, it does not explicitly address flexural hinges that develop adjacent to the column-to-foundation connections similar to beam-to-column connections. Therefore,



**Figure 5.** Assessment results for the panel zones for the CP SPL at the BSE-2 EHL for each archetype building: (a) MC4 ELF design; (b) MC4 RSA design; (c) MC8 ELF design; (d) MC8 RSA design; (e) MC16 ELF design; and (f) MC16 RSA design.

base hinges are evaluated as an “Improved WUF–Welded Web” beam-to-column connection in lieu of a standard column hinge, but with the same  $P - M$  interaction. No reductions were applied to the permissible parameters, as discussed previously in the Beam-to-Column Connections section. In general, column hinges at the base experience inelastic strain demands (flexural hinge yielding corresponds to a  $DCR_N \approx 0.15$ ).

In the case of the four-story frame, the demands are consistently lower than the permissible strengths and deformations. Several base column hinges at the exterior of the 8- and 16-story frames do not satisfy the acceptance criteria because of high axial force and moment. These column hinges are force-controlled for flexure because the axial compression force demand exceeds  $0.5 \times P_{CL}$ , where  $P_{CL}$  is the lower-bound compression strength of the member, which is generally associated with out-of-plane flexural buckling. As such,

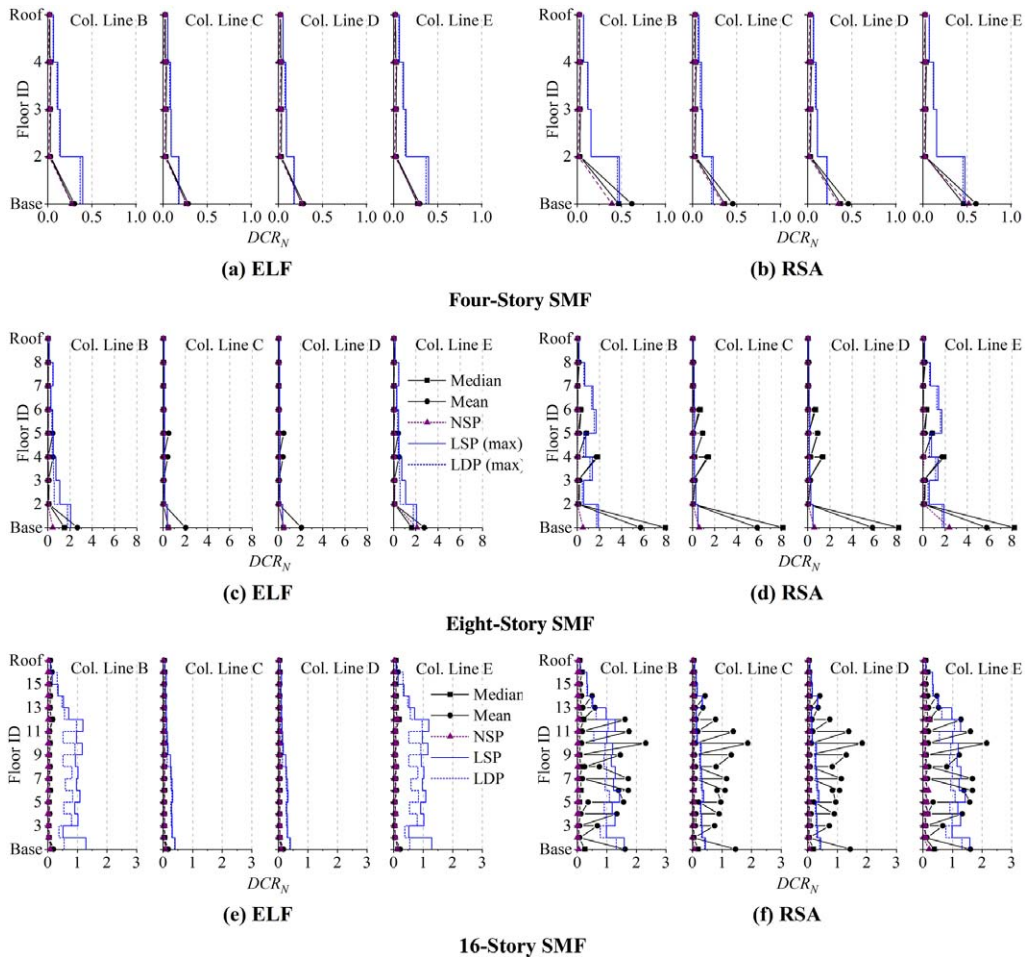


**Figure 6.** Assessment results for the column hinges for the CP SPL at the BSE-2 EHL for each archetype building: (a) MC4 ELF design; (b) MC4 RSA design; (c) MC8 ELF design; (d) MC8 RSA design; (e) MC16 ELF design; and (f) MC16 RSA design.

these columns would need to be evaluated using Equations 2 and 4. Although not explicitly stated in *ASCE 41*, it is assumed here that the flexural action converts to force-controlled in the NDP only during the time steps in which the axial force ratio exceeds 0.5; otherwise, a flexural hinge is permitted to develop in the column. Still, the axial force demand is the result from an individual record and is, therefore, biased by the behavior of the frame to that record. As such, it is difficult to capture record-to-record variability on force- and deformation-controlled response directly in the analysis for a set of ground motion records with this axial load trigger. Taller frames indicate a much wider dispersion of axial load demands, notably when evaluating the RSA-designed frames with the LSP. These results are problematic for assessment because flexure hinges are *expected* to develop at the base of these columns.

Though there is a fundamental difference in how the  $DCR_N$  is computed for the linear and nonlinear procedures, the linear assessment results show similar distributions of demands and location of potential performance concerns. Further, the  $DCR_N$  results for the LSP and LDP are based on an interaction equation and not from the ratio of flexural demand to flexural capacity, which would be a more physically consistent metric for comparison against the results from the nonlinear assessment procedures.

The results for the base columns show the challenges that currently exist for assessment of columns using *ASCE 41*. First, it is of debatable validity that force-controlled response be triggered with  $P_{CL}$  in lieu of  $P_{ye}$ , where  $P_{ye}$  is the expected axial yield capacity of the section, as was used in *FEMA 273*, as inelastic straining is a function of material properties and not member length. Second, the axial-moment interaction formulation in *ASCE 41* used for the case of out-of-plane instability and in-plane flexure is also debatable as it treats flexural yielding of the section and buckling of the member within the same interaction equation. It is theoretically inconsistent to model the component capacities within the same column as a function of both  $P_{ye}$  and  $P_{CL}$ —as well as using  $P_{CL}$  for a column in tension. *ASCE 41* does not provide guidance on checking member stability when using the nonlinear procedures unless the column is designated as force-controlled. Third, experimental tests ([Ozkula et al. 2017a](#)) on deep, shallow wide-flange steel beam-columns commonly used in moment frames showed that the response of plastic hinges from in-plane flexure is not affected by the out-of-plane buckling strength. Out-of-plane buckling patterns were observed in the tests after plastic hinges had developed at both ends of the columns and were proposed to be a function of section compactness and associated local buckling patterns from yielding ([Ozkula et al. 2017b](#)). These tests further showed significant axial shortening within the plastic hinge, a phenomenon that is generally not evaluated in seismic assessments that use phenomenological hinges. Additional research may suggest that the permissible deformations should also be a function of weak-axis geometric properties, that potentially being  $L/r_y$ , where  $L$  is the column length and  $r_y$  is the radius of gyration about the weak-axis ( $y$ -axis), but still an effect of yielding. Lastly, *ASCE 41* would benefit from decoupling the single interaction curve for member stability and section strength into two separate interaction equations as was done in *Chapter N, Plastic Design (AISC 1989)*. Further discussion regarding seismic assessment of columns using *ASCE 41* is provided in [Harris and Speicher \(2015a\)](#).

## SEISMIC ASSESSMENT SUMMARY

*ASCE 41* requires that all frame components not satisfying the acceptance criteria be retrofitted or replaced, even if only a small percentage of the total components fail the criteria. Therefore, a building can only satisfy a selected SPL when all structural components satisfy the respective acceptance criteria. However, building behavior is rarely governed by the response of a single component, with the one notable exception being collapse resulting from compression failure of a primary column. A consequence of a deterministic-type component evaluation (i.e., pass or fail) is that analytical results, depending on the accuracy of the model and analysis algorithms, can be independent of the behavior of the system. Individual member performance and the potential need to retrofit or replace it are therefore based on an analysis output rather than the influence of the component performance on the system performance.

The assessment results show that, on average, the ELF-designed SMF performs better than the RSA-designed SMF for all archetype buildings studied. This can be attributed to the increased strength and stiffness provided to the ELF-designed frames by differences in the design procedures, including associated scaling provisions, in *ASCE 7*. This trend was also observed in collapse analyses of SMFs in *NIST (2010)*. As a side note, *ASCE/SEI 7-16 (2016)* has increased the minimum modal base shear computed using the RSA procedure from 85% to 100% of the base shear computed using the ELF procedure.

### Linear Assessment Procedures

Table 3 summarizes the performance of the archetype buildings in reference to the BSO for both linear procedures. Column performance (primarily at the base) from both assessment procedures controls the overall assessment of the SMF frames.

The LDP consistently results in lower  $DCR_N$  values than the LSP for both the ELF- and RSA-designed frames for all archetype buildings, an indication that a more accurate distribution of seismic demands (based on elastic modes) is better captured in taller frames. Further, assessment of the RSA-designed frame consistently indicates improved performance using the LDP as compared with the LSP because of the variation between the distribution of seismic demands and the allocation of component strengths within the frame. This variation is not as substantial when assessing the ELF-designed frame with the LDP. Moreover, the lateral force distribution in the LSP does not capture higher modes well, leading to conservative estimates of column forces in the taller frames. This can be problematic for columns due to the use of a lower-bound estimate of compressive strength,  $P_{CL}$ .

### Nonlinear Assessment Procedures

Table 4 summarizes the performance of the archetype buildings in reference to the BSO for both nonlinear procedures. Similar to the linear procedures, column hinge performance (primarily at the base) from both assessment procedures controls the overall assessment of the frames. Base column failure in this context is more detrimental to the overall structural performance than beam-to-column connection performance.

**Table 3.** Summary of predicted component performance by the linear procedures for the CP SPL at the BSE-2 EHL for each archetype building

Archetype	Design	LSP			LDP			
		BC <sup>a</sup>	CM <sup>b</sup>	PZ <sup>c</sup>	Design	BC	CM	PZ
4-story	ELF	Fail	Pass	Pass	ELF	Pass	Pass	Pass
	RSA	Fail	Pass	Pass	RSA	Fail	Pass	Pass
8-story	ELF	Pass	Fail	Pass	ELF	Pass	Fail	Pass
	RSA	Fail	Fail	Pass	RSA	Pass	Fail	Pass
16-story	ELF	Pass	Fail	Pass	ELF	Pass	Pass	Pass
	RSA	Fail	Fail	Pass	RSA	Fail	Fail	Pass

<sup>a</sup> BC = Beam-to-column connection.

<sup>b</sup> CM = Column member.

<sup>c</sup> PZ = Panel zone.

**Table 4.** Summary of predicted component performance by the nonlinear procedures for the CP SPL at the BSE-2 EHL for each archetype building

Archetype	Design	NSP			Design	NDP (mean)		
		BC <sup>a</sup>	CH <sup>b</sup>	PZ <sup>c</sup>		BC	CH	PZ
4-story	ELF	Pass	Pass	Pass	ELF	Pass	Pass	Pass
	<b>RSA</b>	<b>Fail</b>	Pass	Pass	<b>RSA</b>	<b>Fail</b>	Pass	Pass
8-story	<b>ELF</b>	Pass	<b>Fail</b>	Pass	<b>ELF</b>	<b>Fail</b>	<b>Fail</b>	Pass
	<b>RSA</b>	Pass	<b>Fail</b>	Pass	<b>RSA</b>	<b>Fail</b>	<b>Fail</b>	<b>Fail</b>
16-story	ELF	Pass	Pass	Pass	ELF	Pass	Pass	Pass
	<b>RSA</b>	Pass	Pass	Pass	<b>RSA</b>	<b>Fail</b>	<b>Fail</b>	Pass

<sup>a</sup> BC = Beam-to-column connection.

<sup>b</sup> CH = Column hinge.

<sup>c</sup> PZ = Panel zone.

The NSP consistently results in lower  $DCR_N$  values than the NDP for both the ELF- and RSA-designed frames for all archetype buildings, an indication that a more accurate distribution of seismic demands is not captured well in taller frames using the NSP. Results indicate that the NSP tends to underestimate the demands in the upper stories compared to the results from the NDP. This occurs primarily because of the differences in the distribution of seismic demands and the lack of modal representation other than the fundamental mode in the NSP.

Results from the NDP are sensitive to excitation input, analysis parameters, and component modeling. In this study, generalized component models were incorporated with stiffness degradation effects calibrated to test data. Experimental research has shown that subassembly tests can have large scatter in acceptable performance given the stochastic variations in the loading and material properties.

Regarding the statistical analysis summarizing the results from the NDP, the response of the beam-to-column connections and panel zones are independent of the direction of the seismic input because the damage mechanism is considered the same in the positive and negative direction. Therefore, the envelop approach of taking the maximum absolute response from each record is valid. Taking the second-floor interior connection (Bay D-E) in the 8-story ELF-designed frame for example—see Table 5—the mean is 2.6 for 14 records. This number is biased by the large response values from Equations 8, 10, and 13. As the damage mechanism is analytically assumed independent of the direction of motion, the same values for positive and negative from the mirrored connection (from symmetry) are computed if the input is reversed. Therefore, statistically speaking, the results can encompass two times the number of records, though the correlation effect of applying the same records in the opposite direction may be an issue. For 28 records, the mean is 2.4 using the envelope approach. If negative and positive values were grouped separately, the mean for 28 records is 1.4 and 1.3, respectively. While these numbers do not change the outcome, it shows the potential sensitivity of the statistical analysis results for a structural component. Additionally, *ASCE 41* is silent as to which statistical distribution is applicable if values other than the mean response (or capacities) are required for assessment.

**Table 5.**  $DCR_N$  values for the interior beam-to-column connection on the second floor of the 8-story ELF-designed SMF (Bay D-E)

EQ	$+DCR_N$	$-DCR_N$	Max
1	<b>0.50</b>	0.21	0.50
2	<b>0.63</b>	0.12	0.63
3	0.42	<b>0.48</b>	0.48
4	0.35	<b>0.60</b>	0.60
5	<b>0.35</b>	0.30	0.35
6	<b>0.45</b>	0.20	0.45
7	<b>0.58</b>	0.18	0.58
8	0.05	<b>11.71</b>	<u>11.71</u>
9	<b>0.46</b>	0.31	0.46
10	0.16	<b>11.29</b>	<u>11.29</u>
11	<b>0.69</b>	0.24	0.69
12	0.05	<b>0.52</b>	0.52
13	0.24	<b>6.30</b>	<u>6.30</u>
14	<b>1.41</b>	0.30	1.41

In contrast to the mean response, the median response generally indicates better performance because it is less influenced by large deformations resulting from component strength loss. The median for the above noted connection is 0.6 for 14 records. Consequently, the median may be a more stable performance metric when analyzing many ground motion records with a few poor performers, but should be restrained relative to the mean value.

### Comparison Between Linear and Nonlinear Assessment Results

Table 6 summarizes the performance of the archetype buildings for each analysis procedure. The results indicate that the linear procedures consistently provide  $DCR_N$  values greater than that given by the nonlinear procedures, highlighting the intentional conservatism in the linear procedures. However, this conservatism is coupled with a reduction in required resources and analytical proficiency. Still, on average, the LSP and LDP can identify potential performance concerns within critical areas of the frame as compared to the results from the NSP and NDP. Consistency of results between the assessment procedures is evident in the

**Table 6.** Summary of predicted performance for the CP SPL at the BSE-2 EHL for each archetype building

Archetype	Design	LSP	LDP	NSP	NDP (mean)
4-story	ELF	<b>Fail</b>	Pass	Pass	Pass
	RSA	<b>Fail</b>	<b>Fail</b>	<b>Fail</b>	<b>Fail</b>
8-story	ELF	<b>Fail</b>	<b>Fail</b>	<b>Fail</b>	<b>Fail</b>
	RSA	<b>Fail</b>	<b>Fail</b>	<b>Fail</b>	<b>Fail</b>
16-story	ELF	<b>Fail</b>	Pass	Pass	Pass
	RSA	<b>Fail</b>	<b>Fail</b>	<b>Fail</b>	<b>Fail</b>

global performance rating of the eight-story SMF, as well as frames designed per the RSA procedure. However, not all component performance failures align between the procedures.

The effects of ground motion selection and scaling can be important for the NDP, including the number of records adopted to achieve a reasonable level of statistical confidence and the method by which the records were selected (without a bias to achieve an unfairly beneficial outcome, i.e., “cherry-picking”). Uribe et al. (2017) showed that ground motion selection using the Conditional Mean Spectrum approach may result in reduced  $DCR_N$  values when compared with some traditional approaches. Moreover, some of the higher mode periods fall directly in localized high energy regions of the response spectrum, resulting in increased demands that cannot be captured efficiently in a linear analysis using a smooth, generalized spectrum. Furthermore, the force distribution used in the NSP is potentially inadequate for frames that exhibit increased higher mode participation, either elastically or triggered by nonlinearity.

The columns that failed the linear assessment criteria are typically force-controlled for flexure because of high axial loads. In comparison with the results from the NDP, the linear procedures produced conservative estimates of poor performance. On average, the linear procedures slightly overestimated the axial force demand in the exterior columns. Although there is general agreement between the procedures on which components may pose a risk, evaluation of the results from the NDP suggests that the columns may satisfy the performance criteria if the hinges were not force-controlled using  $P_{CL}$ .

## CONCLUSIONS

This paper presents the results of a study investigating the correlation between the anticipated seismic performance of an *ASCE 7* code-compliant steel building with special moment frames and its predicted performance as quantified using *ASCE 41* analysis procedures and structural performance metrics. This investigation was performed by evaluating a suite of structural steel buildings located in a high seismicity region designed using *ASCE 7* and evaluated using *ASCE 41*. The basic question is whether the standards for designing new steel buildings and assessing existing steel buildings provide consistent levels of performance. A detailed discussion regarding observation, conclusion, and research needs is provided in Harris and Speicher (2015a).

The following observations and conclusions are based on the collective results obtained from the assessment of the special moment frames:

- Analytical results based on component-level performances indicate that new SMFs designed in accordance with *ASCE 7*, and its referenced standards have difficulty achieving the *ASCE 41* BSO for an existing building intended to be equivalent to a new building.
- Assuming the archetype buildings meet the collapse performance objective of *ASCE 7*, the results of the assessment procedures indicate that *ASCE 41* is generally conservative for SMFs.
- A significant number of columns, primarily at the exterior of the frames, did not satisfy the *ASCE 41* acceptance criteria. These failures are in columns classified by analysis as force-controlled, which can be particularly problematic for assessment

when the columns are located at the base of a frame where flexural hinges are anticipated.

- A significant number of RBS beam-to-column connections, primarily at the exterior of the frames, did not satisfy the *ASCE 41* acceptance criteria. Although the nonlinear acceptance criteria and detailing recommendations in *ASCE 41* were derived from experimental test data, the rationale for the quantitative development of the cumulative reduction factors on these criteria is unclear.
- Assessment results show that panel zones are deemed stronger than required by *ASCE 41*, which adopted the balanced yield approach between beam and panel zone yielding. This is a result of current design procedures, including the practice of upsizing columns to offset the need for doubler plates and/or continuity plates. Consequently, this resulted in reduced permissible capacities of some beam-to-column connections.

The following items are general considerations for future studies to enhance *ASCE 41* assessment provisions:

- The archetype buildings should be analyzed using the methodology formulated in FEMA P695 (FEMA 2009b). This will provide the requisite data to identify the collapse probability of the systems (or frames) in relation to the intended collapse objective of *ASCE 7*. Results from this study can be used to probabilistically relate the *R*-factor in *ASCE 7* to *m*-factors and inelastic deformations using story drift. This work will highlight which standard may not be meeting its intended performance objective and where to concentrate future studies.
- Research is needed to couple the collapse performance objectives of the two standards by investigating the implementation of risk-targeted collapse assessment criteria into *ASCE 41* similar to the design philosophy introduced in *ASCE 7*. As such, comparison of system fragility curves should be done to correlate the risk-target of *ASCE 7* and the risk-target of an existing building intended to be equivalent to a new building.
- Research should be conducted to determine the number of components that do not need to satisfy the *ASCE 41* component acceptance criteria while still permitting the building to be classified as meeting a performance objective.
- Research should evaluate the influence of gravity framing on assessment results of the primary components of the SFRS.
- Research is required to justify updated interaction equations for assessment of columns using *ASCE 41*. Decoupling interaction equations into specific failure mechanisms and referencing vetted design standards should be considered. Removing  $P_{CL}$  as the basis for force-controlled response and permissible capacities used to assess a flexural hinge should also be considered. Work is needed regarding column-to-foundation connections.
- Research should critically examine the applicability of the generalized modeling parameters in *ASCE 41* for nonlinear actions in components of steel moment frames for use in the nonlinear procedures—see NIST (2017b). This should include the influence of the loading protocol adopted to establish the permissible capacities.

## DISCLAIMER

Certain commercial software, equipment, instruments, or materials may have been used in the preparation of information contributing to this paper. Identification in this paper is not intended to imply recommendation or endorsement by NIST, nor is it intended to imply that such software, equipment, instruments, or materials are necessarily the best available for the purpose.

No formal investigation to evaluate potential sources of uncertainty or error, or whether multiple sources of error are correlated, was included in this study. The question of uncertainties in the analytical models, solution algorithms, material properties and as-built dimensions and positions of members versus design configurations employed in analysis are beyond the scope of the work reported here.

## REFERENCES

- American Institute of Steel Construction (AISC), 1989. *Specification for Structural Steel Buildings: Allowable Stress Design and Plastic Design*, Chicago, IL.
- American Institute of Steel Construction (AISC), 2010a. *Specification for Structural Steel Buildings, ANSI/AISC 360-10*, Chicago, IL.
- American Institute of Steel Construction (AISC), 2010b. *Seismic Provisions for Structural Steel Buildings, ANSI/AISC 341-10*, Chicago, IL.
- American Institute of Steel Construction (AISC), 2010c. *Prequalified Connections for Special and Intermediate Steel Moment Frames for Seismic Applications, ANSI/AISC 358-10*, Chicago, IL.
- American Institute of Steel Construction (AISC), 2011. *Steel Construction Manual*, 14 Ed., Chicago, IL.
- American Society of Civil Engineers (ASCE), 2007. *Seismic Rehabilitation of Existing Buildings, ASCE/SEI 41-06*, Reston, VA.
- American Society of Civil Engineers (ASCE), 2010. *Minimum Design Loads for Buildings and Other Structures, ASCE/SEI 7-10*, American Society of Civil Engineers, Reston, VA.
- American Society of Civil Engineers (ASCE), 2014. *Seismic Evaluation and Retrofit of Existing Buildings, ASCE/SEI 41-13*, Reston, VA.
- American Society of Civil Engineers (ASCE), 2016. *Minimum Design Loads for Buildings and Other Structures, ASCE/SEI 7-16*, Reston, VA.
- American Society of Civil Engineers (ASCE), 2017. *Seismic Evaluation and Retrofit of Existing Buildings, ASCE/SEI 41-17*, Reston, VA.
- American Society for Testing and Materials (ASTM), 2013. *A500/A500M-13 Standard Specification for Cold-Formed Welded and Seamless Carbon Steel Structural Tubing in Rounds and Shapes*, ASTM International, West Conshohocken, PA.
- American Society for Testing and Materials (ASTM), 2015a. *A992/A992M-11 Standard Specification for Structural Steel Shapes*, ASTM International, West Conshohocken, PA.
- American Society for Testing and Materials (ASTM), 2015b. *A572/A572M-15 Standard Specification for High-Strength Low-Alloy Columbium-Vanadium Structural Steel*, ASTM International, West Conshohocken, PA.

- California Building Standards Commission (CBSC), 2010. *California Code of Regulations, Part 2 – California Building Standards Code – Title 24*, Sacramento, CA.
- Computers and Structures, Inc. (CSI), 2011a. ETABS (Version 9.7.4), software, Berkeley, CA.
- Computers and Structures, Inc. (CSI), 2011b. PERFORM-3D (Version 5.0), software, Berkeley, CA.
- Federal Emergency Management Agency (FEMA), 1997. *NEHRP Guidelines for the Seismic Rehabilitation of Buildings*, FEMA 273, Washington, D.C.
- Federal Emergency Management Agency (FEMA), 2000a. *Prestandard and Commentary for the Seismic Rehabilitation of Buildings*, FEMA 356, Washington, D.C.
- Federal Emergency Management Agency (FEMA), 2000b. *State of the Art Report on Connection Performance*, FEMA 355D, Washington, D.C.
- Federal Emergency Management Agency (FEMA), 2009a. *NEHRP Recommended Seismic Provisions for New Buildings and Other Structures*, FEMA P-750, Washington, D.C.
- Federal Emergency Management Agency (FEMA), 2009b. *Quantification of Building Seismic Performance Factors*, FEMA P695, Washington, D.C.
- U.S. General Services Administration (GSA), 2012. *Facilities Standards for the Public Buildings Service*, PBS-P100, Washington, D.C.
- Harris, III, J. L., and Speicher, M. S., 2015a. *Assessment of First Generation Performance-Based Seismic Design Methods for New Steel Buildings, Volume 1: Special Moment Frames*, NIST TN 1863-1, National Institute of Standards and Technology, Gaithersburg, MD, p. 299, <http://dx.doi.org/10.6028/NIST.TN.1863-1> (last accessed 22 August 2018).
- Harris, III, J. L., and Speicher, M. S., 2015b. *Assessment of First Generation Performance-Based Seismic Design Methods for New Steel Buildings, Volume 2: Special Concentrically Braced Frames*, NIST TN 1863-2, National Institute of Standards and Technology, Gaithersburg, MD, p. 267, <http://dx.doi.org/10.6028/NIST.TN.1863-2> (last accessed 22 August 2018).
- Harris, III, J. L., and Speicher, M. S., 2015c. *Assessment of First Generation Performance-Based Seismic Design Methods for New Steel Buildings, Volume 3: Eccentrically Braced Frames*, NIST TN 1863-3, National Institute of Standards and Technology, Gaithersburg, MD, p. 279, <http://dx.doi.org/10.6028/NIST.TN.1863-3> (last accessed 22 August 2018).
- International Code Council (ICC), 2012a. *International Existing Building Code (IEBC)*, Washington, D.C.
- International Code Council (ICC), 2012b. *International Building Code (IBC)*, Washington, D.C.
- Krawinkler, H., 1978. Shear in beam-column joints in seismic design of steel frames, *AISC Engineering Journal* **15**, 82–91.
- National Institute of Building Sciences (NIBS), 2013. *National Performance-Based Design Guide for Buildings*, Washington, D.C.
- National Institute of Standards and Technology (NIST), 2010. *Evaluation of the FEMA P-695 Methodology for Quantification of Building Seismic Performance Factors*, NIST GCR 10-917-8, Produced by the NEHRP Consultants Joint Venture, a partnership of the Applied Technology Council and the Consortium of Universities for Research in Earthquake Engineering, for the NIST, Gaithersburg, MD, p. 268, available at <http://www.nehrp.gov/pdf/nistgcr10-917-8.pdf> (last accessed 22 August 2018).
- National Institute of Standards and Technology (NIST), 2011. *Standards of Seismic Safety for Existing Federally Owned and Leased Buildings: ICSSC Recommended Practice (RP) 8*, NIST GCR 11-917-12, Produced by the Building Seismic Safety Council of the National Institute of

- Buildings Sciences for NIST, Gaithersburg, MD, p. 39, available at <http://www.nehrp.gov/pdf/nistgcr11-917-12.pdf> (last accessed 22 August 2018).
- National Institute of Standards and Technology (NIST), 2012. *Tentative Framework for Development of Advanced Seismic Design Criteria for New Buildings, NIST GCR 12-917-20*, Produced by the NEHRP Consultants Joint Venture, a partnership of the Applied Technology Council and the Consortium of Universities for Research in Earthquake Engineering, for NIST, Gaithersburg, MD, p. 302, available at <http://www.nehrp.gov/pdf/nistgcr12-917-20.pdf> (last accessed 22 August 2018).
- National Institute of Standards and Technology (NIST), 2017a. *Implementation Guidelines for Executive Order 13717: Establishing a Federal Earthquake Risk Management Standard: ICSSC Recommended Practice (RP) 9, NIST TN 1922*, Gaithersburg, MD, p. 57, <http://doi.org/10.6028/NIST.TN.1922> (last accessed 22 August 2018).
- National Institute of Standards and Technology (NIST), 2017b. *Recommended Modeling Parameters and Acceptance Criteria for Nonlinear Analysis in Support of Seismic Evaluation, Retrofit, and Design – NIST GCR 17-917-45*, produced by the Applied Technology Council for NIST, Gaithersburg, MD, available at <https://nvlpubs.nist.gov/nistpubs/gcr/2017/NIST.GCR.17-917-45.pdf>.
- Ozkula, G., Harris, J., and Uang, C. M., 2017a. Observations from cyclic tests on deep, wide-flange beam-columns, *AISC Engineering Journal* **54**(1), 45–59.
- Ozkula, G., Harris, J., and Uang, C. M., 2017b. Classifying cyclic buckling modes of steel wide-flange columns, *Proceedings of the Structures Congress 2017*, 6–7 April 2017, Denver, CO.
- Speicher, M. S., and Harris, J. L., 2016a. Collapse prevention seismic performance assessment of new eccentrically braced frames using ASCE 41, *Engineering Structures* **117**, 344–357.
- Speicher, M. S., and Harris, J. L., 2016b. Collapse prevention seismic performance assessment of new special concentrically braced frames using ASCE 41, *Engineering Structures* **126**, 652–666.
- Speicher, M. S., and Harris, J. L., 2017. ASCE/SEI 41 predicted performance of newly designed BRBFs, Paper No. 2424, in *Proceedings of the 16th World Conference on Earthquake Engineering*, 9–13 January 2017, Santiago, Chile.
- Uribe, R., Sattar, S., and Speicher, M. S., 2017. Influence of ground motion selection on the assessment of a steel special moment frame, Paper No. 2410, in *Proceedings of the 16th World Conference on Earthquake Engineering*, 9–13 January 2017, Santiago, Chile.

(Received 1 May 2017; accepted 26 February 2018)